ELSEVIER

Polymer 42 (2001) 8235–8239

polymer

www.elsevier.nl/locate/polymer

Polyamide 6-clay nanocomposites/polypropylene-grafted-maleic anhydride alloys

Xiaohui Liu[a], Qiuju Wu[a], Lars A. Berglund[a,*], Jiaqi Fan[b], Zongneng Qi[b]

[a]*Division of Polymer Engineering, Luleå University of Technology, 971 87 Lulea, Sweden*
[b]*State Key Laboratory of Engineering Plastics, Institute of Chemistry, Chinese Academy of Sciences, Beijing 100080, People's Republic of China*

Received 4 December 2000; received in revised form 20 April 2001; accepted 25 April 2001

Abstract

Polyamide 6-clay nanocomposites (PA6CN) based on montmorillonite typically show some brittleness with clay addition. In order to address this problem, PA6CN/PP-g-MAH alloys were prepared through blending PA6CN with polypropylene-grafted-maleic anhydride (PP-g-MAH). The mechanical properties, dynamic mechanical temperature spectra, morphology and water absorption of the alloys were studied. Compared with PA6CN, the notched impact strength of the alloys increased greatly while the alloys still maintained higher stiffness and strength than that of PA 6. The morphological studies via scanning electron microscopy (SEM) showed a PP-g-MAH toughen phase dispersed in PA6CN matrix. As the PP-g-MAH content was increased, reduced water absorption was observed.

Keywords: PCN/PP-g-MAH alloys; Mechanical properties; Dynamic mechanical temperature spectra

1. Introduction

In recent years, organic–inorganic nanoscale composites have attracted great interest since they frequently exhibit unexpected hybrid properties synergistically derived from two components [1–17]. One of the most promising composites systems would be the hybrid based on organic polymers and inorganic clay minerals consisting of layered silicates. Because of the nanoscale structure, nanocomposites possess unique properties typically not shared by conventional microcomposites. As a consequence, there are interesting opportunities for the development of new technology [1]. Polyamide 6-clay nanocomposites (PA6CN) based on montmorillonite is a successful example [8–10]. This kind of nanocomposites showed a near doubling of modulus and strength in materials containing as little as 4.2 wt% clay. The heat distortion temperature (HDT) increased from 65°C of polyamide 6 up to 150°C of the nanocomposites.

Although dramatic improvement was observed in modulus, strength and heat resistance, the PA6CN was more brittle than PA 6.

In this context, we considered the extensive literature on polyamide alloys with various toughening polymers including thermoplastics, elastomers and rubbers [18–34]. Generally speaking, most combinations are immiscible. A compatibilizer, which is able to improve interfacial interaction between the polymers is desirable. For example, maleic anhydride grafted rubbers are commonly used compatibilizers for polyamide alloys. Despite the extensive literature on polyamide alloys, we have not found reports about alloy systems using PA6CN as matrix.

In the present work, we report the preparation of PA6CN/PP-g-MAH alloys and investigate the mechanical and dynamic mechanical properties, morphologies and water absorption of these materials.

2. Experiment

2.1. Materials

The PA6CN was synthesized in a reaction vessel according to the methods described in Refs. [8–10]. The Na-montmorillonite used to prepare the PA6CN was a natural clay mineral with a cation exchange capacity of 79 mequiv/100 g, the mean size of the clay particles was 40 μm. For preparing PA6CN containing 5 wt% montmorillonite, in 1 L of water, Na-montmorillonite (40 g) was dispersed at 50°C for 8 h. ϵ-Caprolactam (800 g), phosphoric acid, and 6-aminocaproic acid were added in the montmorillonite

* Corresponding author. Tel.: +46-920-91580; fax: +46-920-910-84.
E-mail address: lars.berglund@mb.luth.se (L.A. Berglund).

0032-3861/01/$ - see front matter
PII: S0032-3861(01)00307-X

Table 1
Mechanical and thermal properties of the PA6CN and PA 6

Properties	PA6CN (5 wt% clay content)	PA 6
Tensile strength (MPa)	88.60	52.32
Tensile modulus (GPa)	2.52	1.80
Flexural strength (MPa)	138.60	84.98
Flexural modulus (GPa)	2.87	1.64
Notched Izod impact strength (J/m)	23	39
HDT (°C) (1.82 MPa)	152	65

dispersion [10]. The mixture was allowed to react at 260°C for 6 h in N_2 atmosphere under normal pressure. After completion of the reaction, the product was cooled and cut into granules. The granules were washed with water and then dried in vacuum oven at 80°C for 24 h to obtain PA6CN.

PA 6 was also synthesized as a reference material. Polypropylene-grafted-maleic anhydride (PP-g-MAH) containing 1 wt% maleic anhydride was prepared in our lab.

A twin-screw extruder was used for the preparation of PA6CN/PP-g-MAH alloys. The PA6CN granules were dried in a vacuum oven at 120°C for 24 h prior to blending. The temperature of the extruder was maintained at 220, 245, 245 and 230°C from hopper to die. The screw speed was maintained at 180 rpm. After drying at 80°C for 6 h, the alloys were injection molded to obtain test specimens for measurement of mechanical properties, dynamic mechanical properties and water absorption.

2.2. Characterization

Prior to testing, all specimens were dried in a vacuum oven at 80°C for 24 h. The tensile tests were carried using a universal tensile tester (INSTRON 8501) and the notched Izod impact strength was measured using a pendulum impact tester (CS-137D-167, Custom Scientific Instruments). Tests were performed according to the respective ASTM standards.

The dynamic mechanical analysis was performed using a dynamic mechanical analyzer (Perkin–Elmer DMA-7). The testing was carried out in 3-point bending mode at a vibration frequency of 1 Hz in a temperature range from −160 to 170°C at a heating rate of 5°C/min in a nitrogen atmosphere.

The PCN/PP-g-MAH specimens were fractured at liquid nitrogen temperature and then fracture surfaces were gold coated and observed in a scanning electron microscope (Hitachi H-530).

The water absorption experiments were performed to provide a rough estimate of this characteristic. The molded specimens were kept in deionized, boiling water for a fixed time and then they were quickly placed between sheets of paper to remove the excess water. The amount of absorbed water was calculated from the specimen weight increase. The specimens had the following dimensions: length 50 mm, width 12.7 mm, and thickness 3 mm.

3. Results and discussion

3.1. Properties of the PA6CN

According to the method described in the experimental section, we prepared PA6CN containing 5 wt% montmorillonite. The mechanical properties and HDTs were measured. In Table 1, results are presented for PA6CN and PA 6. The nanometeric dispersion of silicate layers in matrix leads to significantly improved modulus and strength. The stiffness of the silicate layers contributes to the presence of immobilized or partially immobilized polymer phases, those phases have been thoroughly discussed by Eisenberg [35]. It is also possible that silicate layer orientation as well as molecular orientation contribute to the observed reinforcement effects. The HDT increases significantly, as was observed previously [8–10]. Impact strength is somewhat reduced as montmorillonite is added.

3.2. Mechanical properties of the PCN/PP-g-MAH alloys

The mechanical properties of the PA6CN/PP-g-MAH alloys, such as yield strength (σ_y), tensile modulus (E_y), flexural strength (σ_f) and flexural modulus (E_f) are reported in Table 2. The results show that σ_y, E_y, σ_f and E_f decrease with increasing PP-g-MAH content. But compared with PA 6, the PA6CN/PP-g-MAH alloys still exhibit improved properties. Even containing as high as 30 wt% PP-g-MAH, the above properties of the alloys are still higher

Table 2
Properties of the PA6CN/PP-g-MAH alloys

Properties	PA6CN/PP-g-MAH (wt/wt) = 100/0	90/10	80/20	70/30	0/100
Tensile strength (MPa)	88.60	85.06	81.51	74.42	22.83
Tensile modulus (GPa)	2.52	2.39	2.22	2.14	0.91
Flexural strength (MPa)	138.60	128.90	123.35	115.04	28.90
Flexural modulus (GPa)	2.87	2.67	2.58	2.41	0.74
Elongation at break (%)	36	66	101	122	230
Notched Izod impact strength (J/m)	23	61	90	129	49

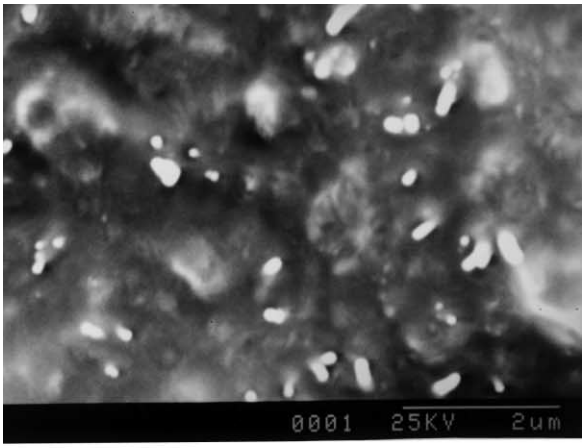

(a)

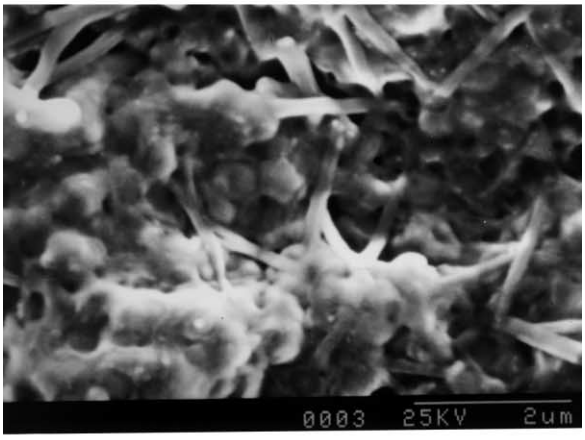

(b)

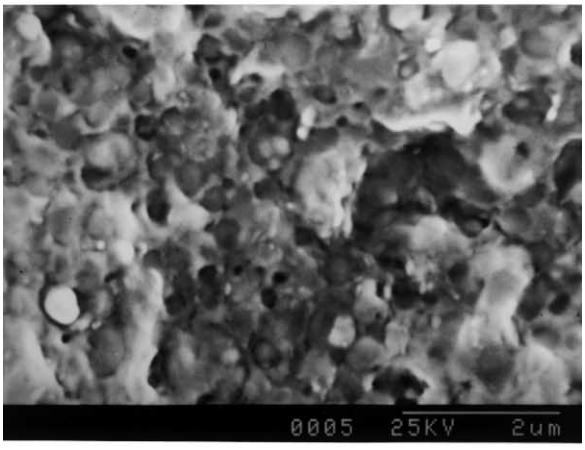

(c)

Fig. 1. SEM micrographs of the alloys: (a) containing 10 wt% PP-g-MAH; (b) containing 20 wt% PP-g-MAH; (c) containing 30 wt% PP-g-MAH.

than that of PA 6. The notched Izod impact strengths (S_I) of the alloys are also shown in Table 2. Already at 10 wt% of PP-g-MAH, the impact strength of alloy (61 J/m) is higher than that of PA 6 (39 J/m), let alone PA6CN (23 J/m). When containing 30 wt% PP-g-MAH, S_I increases up to 129 J/m. The PP-g-MAH addition is able to compensate for the embrittlement caused by the montmorillonite.

In this case, the normal concept of using functional PP as the toughing phase to the PA 6 matrix was applied. The difference compared with the normal alloys is that a higher performance matrix, PA6CN, was selected. Thus, we can obtain an engineering plastic with enough stiffness and toughness for technological applications.

3.3. Morphology

Scanning electron microscopy (SEM) micrographs of the fracture surfaces are presented in Fig. 1. In the case of 90/10 PA6CN/PP-g-MAH, the average PP-g-MAH particle size is smaller than 0.5 μm and the particles are in irregular shapes. For 80/20 PA6CN/PP-g-MAH, 0.1 μm diameter microfibers are observed, they consist of PP-g-MAH formed during extrusion due to the shear forces and the difference in viscosity between the two components. At higher PP-g-MAH content, this simple method is unable to clarify the phase morphologies since the phase separation is not clearly observed at the scale of observation.

The fine dispersion of particles at low PP-g-MAH content already shows the favourable effect arising from compatibilization of the second phase. Stronger phase interactions are also expected to improve interfacial characteristics.

3.4. Dynamic mechanical properties

Dynamic storage modulus (E'), dynamic loss modulus (E'') and the loss factor ($\tan\delta$) versus temperature are plotted in Fig. 2. In the E' curves (Fig. 2a), differences between PA6CN (curve 2) and PP-g-MAH (curve 1) are apparent. With decreasing PA6CN content, the dynamic storage modulus of the alloys decreases. In the E'' curves (Fig. 2b) and tan δ curves (Fig. 2c), PP-g-MAH (curve 1) shows three dynamic relaxation peaks. The dominant relaxation appearing at 0°C is the glass-rubber relaxation of amorphous portions of the PP-g-MAH solid. The less intensive and broader peak at around −60°C can be considered as the γ relaxation, which is attributed to a relaxing unit consisting of a few chain segments rather than involving the motion of PP-g-MAH main chain. The weak peak appearing as a shoulder at about 70°C is associated with the crystalline regions of PP-g-MAH. Fig. 2b and c also show two relaxation peaks of the PA6CN (curve 2). The largest peak at 50°C is the glass transition caused by the movement of large-chain segments, while the peak at about −80°C is associated with crankshaft-type motion involving the unbonded amide group and several methylene carbon groups [31]. The glass transition peak of PP-g-MAH is completely absent in all the alloy compositions. The alloys all show very similar curve with PA6CN. For 70/30 PA6CN/PP-g-MAH alloy, a slight shift towards higher temperature is observed for the secondary relaxation peak at about −80°C. In a summary, we see little signs of any

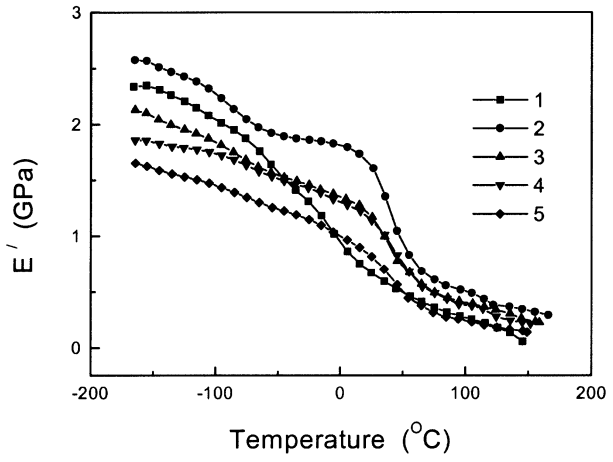

(a)

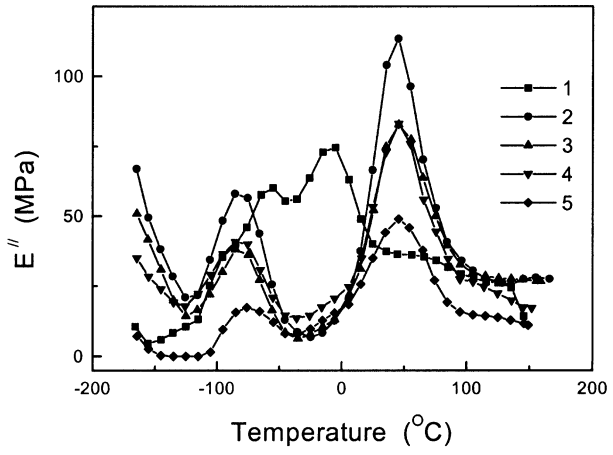

(b)

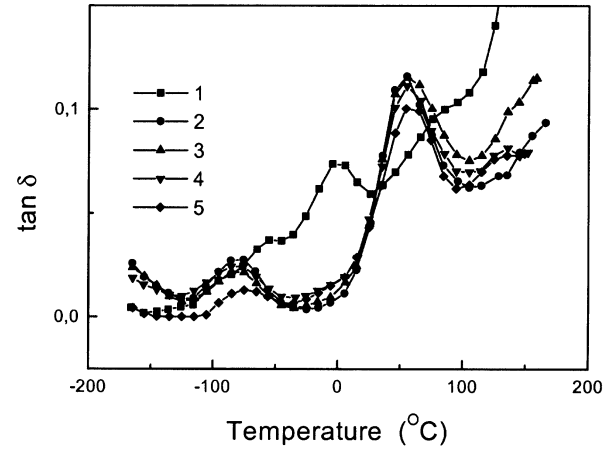

(c)

Fig. 2. Dynamic mechanic spectra of the alloys: (a) temperature dependence of E'; (b) temperature dependence of E''; (c) temperature dependence of tan δ; where (1) PA6CN/PP-g-MAH = 0/100; (2) PA6CN/PP-g-MAH = 100/0; (3) PA6CN/PP-g-MAH = 90/10; (4) PA6CN/PP-g-MAH = 80/20; (5) PA6CN/PP-g-MAH = 70/30.

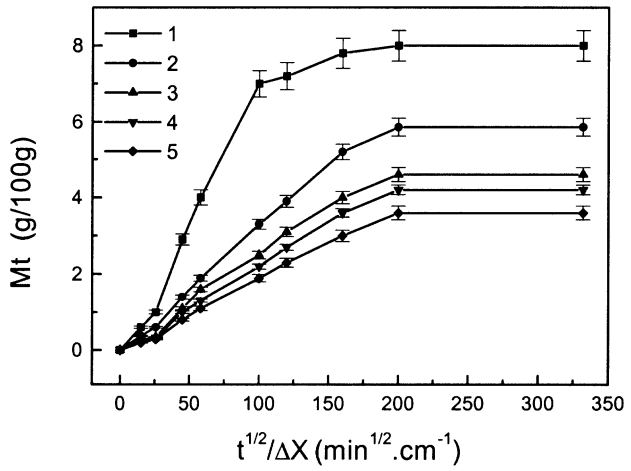

Fig. 3. Water absorption curves: (1) PA 6; (2) PA6CN; (3) PA6CN/PP-g-MAH = 90/10; (4) PA6CN/PP-g-MAH = 80/20; (5) PA6CN/PP-g-MAH = 70/30.

influence from the PP-g-MAH phase on the alloys. The materials must be considered as phase separated blends and PP-g-MAH plays the role of a dispersed phase which toughens the alloys.

3.5. Water absorption of alloys

Water absorption curves may be represented by the weight percent (M_t) of water absorbed in the specimen versus the square root of time divided by the thickness [36]. Fig. 3 shows such absorption curves. All curves show a nearly linear increase at the initial stage, followed by unchanged values after apparent saturation by water. The amount of water absorption in PA6CN is much less than that of PA 6, there is a 2 wt% difference in the saturation value. One reason must be the presence of immobilized and partially immobilized polymer in the amorphous phase. The general concept of these phases has been discussed by Eisenberg [35]. The 70/30 PA6CN/PP-g-MAH alloy

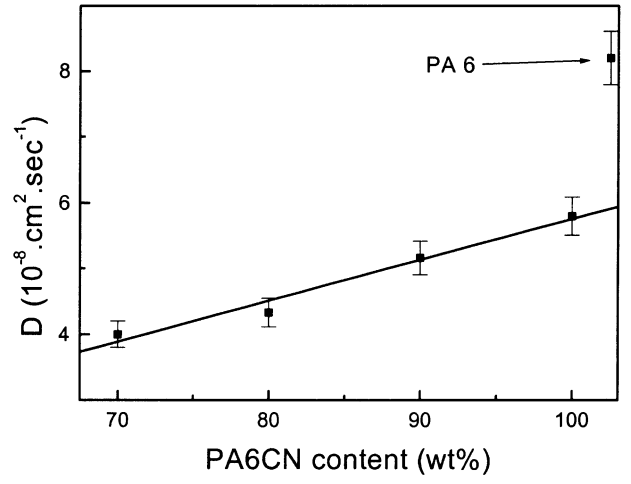

Fig. 4. D as a function of PA6CN content.

absorbs less than half the amount of water of PA 6. The reason is obviously the lack of water absorption in the nonpolar PP region.

The diffusion coefficient is estimated from the absorption data at an early stage (1 h) using

$$M_t/M_\infty = (4/\pi^{1/2})(1/\Delta X)(Dt)^{1/2} \quad (1)$$

where ΔX is the thickness of the specimen, M_t and M_∞ is the amount of water absorbed in specimens at time t and after an infinite time, respectively. The diffusion coefficients thus obtained are presented in Fig. 4. D values decrease with an increase in the amount of PP-g-MAH, and D for PA6CN is less than 75% of that for PA 6.

In addition to the immobilized phase explanation, the presence of crystallites or other impermeable particles obviously also lowers the overall rate of transport. It has also been suggested that impermeable phases increase the average diffusion path length [36].

4. Conclusions

The reduced impact strength of PA6CN nanocomposites with montmorillonite addition was counteracted by blending with PP-g-MAH. Already at 90/10 PA6CN/PP-g-MAH, the original impact strength of PA 6 was exceeded. The PP-g-MAH phase was finely dispersed at a scale smaller than 1 μm at concentrations of 10 and 20 wt%. Tan δ versus temperature data support strong phase separation in the alloys although at a fine scale. The water absorption of PA 6 was reduced by 25% as 5 wt% montmorillonite was added. When containing 20 wt% of PP-g-MAH, the alloy absorbed about 50% water compared with PA 6.

References

[1] Giannelis EP. Adv Mater 1993;8:29.
[2] Krishnamoorti R, Giannelis EP. Macromolecules 1997;30:4097.
[3] Vaia RA, Giannelis EP. Macromolecules 1997;30:8000.
[4] Balazs AC, Singh C, Zhulina E. Macromolecules 1998;31:8370.
[5] Lyatskaya Y, Balazs AC. Macromolecules 1998;31:6676.
[6] Novak BM. Adv Mater 1993;6:422.
[7] Lu S, Melo MM, Zhao J, Pearce EM, Kwei TK. Macromolecules 1995;28:4908.
[8] Usuki A, Kawasumi M, Kojima Y, Fukushima Y, Okada A, Kurauchi T, Kamigaito O. J Mater Res 1993;8:1179.
[9] Kojima Y, Usuki A, Kawasumi M, Kojima Y, Fukushima Y, Okada A, Kurauchi T, Kamigaito O. J Mater Res 1993;8:1185.
[10] Kojima Y, Usuki A, Kawasumi M, Kojima Y, Fukushima Y, Okada A, Kurauchi T, Kamigaito O. J Polym Sci, Part A: Polym Chem 1993;31:1755.
[11] Wang MS, Pinnavaia TJ. Chem Mater 1994;6:468.
[12] Lan T, Pinnavaia TJ. Chem Mater 1994;6:2216.
[13] Kelly P, Akelah A, Qutubuddin S, Moet A. J Mater Sci 1994;29:2274.
[14] Vaia RA, Isii H, Giannelis EP. Chem Mater 1993;5:1694.
[15] Moet A, Akelah A. Mater Lett 1993;18:97.
[16] Messersmith PB, Giannelis EP. J Polym Sci, Part A: Polym Chem 1995;33:1047.
[17] Biasci L, Aglietto M, Ruggeri G, Ciardelli F. Polymer 1994;35:3296.
[18] Bucknall CB. Toughened plastics. London: Applied Science, 1977.
[19] Hobbs SY, Bopp RC, Watkins VH. Polym Engng Sci 1983;23:380.
[20] Wu S. Polymer 1985;26:1855.
[21] Mborggreve RJ, Gaymans RJ, Schuijer J, Ingen Housz JF. Polymer 1987;28:1489.
[22] Lawson DF, Hergenrother WL, Matlock MG. J Appl Polym Sci 1990;39:2331.
[23] Oshinski AJ, Keskkula H, Paul DR. Polymer 1992;33:268.
[24] Oshinski AJ, Keskkula H, Paul DR. Polymer 1992;33:284.
[25] Gilmore DW, Modic MJ. Plastic Engng 1989;April:29.
[26] Wu S. J Polym Sci, Polym Phys Ed 1983;21:699.
[27] Wu S. J Appl Polym Sci 1988;30:549.
[28] Wu S. Polym Engng Sci 1990;30:753.
[29] Liang ZZ, Williams HL. J Appl Polym Sci 1992;44:699.
[30] Sathe SN, Devi S, Srinivasa GS, Rao KV. J Appl Polym Sci 1996;61:97.
[31] Wu CJ, Kuo JF, Chen CY, Woo E. J Appl Polym Sci 1994;52:1695.
[32] Hietaoja PT, Holsti-mittinen RM, Seppala JV, Ikkala OT. J Appl Polym Sci 1994;54:1613.
[33] Duvall J, Sellitti C, Myers C, Hiltner A, Baer E. J Appl Polym Sci 1994;52:195.
[34] Lu M, Keskkula H, Paul DR. J Appl Polym Sci 1995;58:1175.
[35] Tsagaropoulos G, Eisenberg A. Macromolecules 1995;28:6067.
[36] Kojima Y, Usuki A, Kawasumi M, Okada A, Kurauuchi T, Kamigaito O. J Appl Polym Sci 1993;49:1259.